Journal of Earthquake Engineering

ISSN: (Print) (Online) Journal homepage: https://www.tandfonline.com/loi/ueqe20

One-Story Three-Dimensional Frame Structures Behavior Strengthened with External Shear Wall under Cyclic Loading: An Experimental Study

Hurmet Kucukgoncu & Fatih Altun

To cite this article: Hurmet Kucukgoncu & Fatih Altun (2021): One-Story Three-Dimensional Frame Structures Behavior Strengthened with External Shear Wall under Cyclic Loading: An Experimental Study, Journal of Earthquake Engineering, DOI: 10.1080/13632469.2021.1964642

To link to this article: https://doi.org/10.1080/13632469.2021.1964642

Published online: 22 Aug 2021.

JOURNAL OF EARTHQUAKE ENGINEERING
https://doi.org/10.1080/13632469.2021.1964642

Taylor & Francis
Taylor & Francis Group

One-Story Three-Dimensional Frame Structures Behavior Strengthened with External Shear Wall under Cyclic Loading: An Experimental Study

Hurmet Kucukgoncu [a] and Fatih Altun [b]

[a]Department of Civil Engineering, Abdullah Gül University, Kayseri, Turkey; [b]Department of Civil Engineering, Erciyes University, Kayseri, Turkey

ABSTRACT

In this study, the seismic behaviors of strengthened three-dimensional frames, as in real-life structures, are presented. Three reinforced concrete (RC) frames, containing common structural deficiencies were constructed to represent existing older structures. The bare, damaged, and undamaged frames, strengthened by RC external shear walls with steel tie beams, were tested under a reversed cyclic load. The experimental results indicated that strengthening by external shear walls made significant contributions to the frames in lateral strength, stiffness, and energy dissipation capacity. This proposed method appears to be an efficient technique for strengthening structures in an effective, economical, and practical way.

ARTICLE HISTORY
Received 14 April 2020
Accepted 5 July 2021

KEYWORDS
Cyclic loading; exterior shear wall; structural behavior; strengthening; three-dimensional frame

1. Introduction

Many reinforced concrete structures, which have been built in active earthquake zones, have suffered extensive damage or collapsed in past earthquakes (Bal et al. 2008; Damcı et al. 2015; Gunes 2015; Martinelli et al. 2008; Menoni 2001; Miura et al. 2008; Sharma, Deng, and Noguez 2016; Spence et al. 2003; Yakut et al. 2005). Investigations after these earthquakes revealed that these structures did not have adequate strength, lateral stiffness, and ductility (Elnashai 2000; Hassan and Sozen 1997; Sezer et al. 2003). In addition, it was observed that most of the buildings, which were not damaged totally after the earthquakes and were still in use, were constructed with some deficiencies, which caused insufficient seismic performance (Cogurcu 2015; Yön, Sayın, and Onat 2017). These deficiencies were low-quality steel and concrete, faulty workmanship, inadequate design and structural systems, such as flexible columns, soft stories, strong beam–weak column joints, and non-seismic reinforcement details for seismic loading. For this reason, various strengthening methods are applied to prevent serious loss of life, asset losses and to improve the earthquake behavior of reinforced concrete structures (Bal et al. 2008; Calvi 2013; Elnashai and Pinho 1998).

Many strengthening techniques are available depending upon the various types and conditions of existing structures in terms of their seismic performances. These techniques are commonly classified as local and global strengthening approaches. The local strengthening approach is based on increasing the deformation capacities of components so that the ductility of components with inadequate capacities satisfies their specific limit states (Moehle 2000). In this approach, structural members, especially beams and columns, are strengthened by adding concrete, steel, or Fiber composite/Fiber reinforced polymer (FRP/CFRP) jackets (Bousias, Spathis, and Fardis 2007; Furuta, Kanakubo, and Fukuyama 2003; Ghobarah, Biddah, and Mahgoub 1997; Ghosh and Sheikh 2007; Oehlers 1990; Ozcan, Binici, and Ozcebe 2008; Saadatmanesh, Ehsani, and Li 1994; Spadea, Bencardino, and Swamy

CONTACT Hurmet Kucukgoncu hurmet.kucukgoncu@agu.edu.tr Department of Civil Engineering, Abdullah Gül University, Kayseri 38080, Turkey

1998; Tzoura and Triantafillou 2016; Ye et al. 2002). These studies showed that such strengthening methods increased the deformation capacities of structural members, and they provided an improvement in the ductile behavior of the members to prevent them from undergoing brittle failure under seismic effects.

The global strengthening approach is considered for improvements of all structural systems in terms of increasing the load carrying capacity by providing enough strength and lateral stiffness (Çırak et al. 2015). Among these methods, the addition of reinforced concrete or steel shear walls inside the structure is the most commonly used for structural systems (Amjad et al. 2003; Altin et al. 2008; Anil, Altin, and Kara 2008; Aoyama et al. 1984; Badoux and Jirsa 1990; Canbay, Ersoy, and Ozcebe 2003; Erdem et al. 2006; Frosch et al. 1996; Ismaeil and Hassaballa 2013; Phan, Cheok, and Todd 1995; Pujol and Fick 2010; Sonuvar, Ozcebe, and Ersoy 2004; Türk, Ersoy, and Özcebe 2003). In these studies, adding infill walls inside the structural system significantly contributes to increasing the lateral strength and stiffness. Although many strengthening methods have been developed with the improvement of technology and experimental opportunities in recent years, most of these methods seem difficult to be applied practically. Many of them require the evacuation of a structure during rehabilitation and they are both time-consuming and lead to additional heavy costs, especially for official buildings (schools, hospitals, etc.), which are important to maintain their functions during the strengthening application. The objective of this research was to develop a more practical, efficient, and economical method that will not interrupt the usage of buildings for strengthening of reinforced concrete structural systems by adding external shear walls to the exterior sides of the structure. Although some research was conducted on strengthening frames by using external shear walls, the frame specimens strengthened with external shear walls were constructed in two dimensions in these studies (Görgülü et al. 2012; Kaltakci, Arslan, and Yilmaz 2011; Ozturk 2010; Ünal 2012).

In a study by Ozturk (2010), an external shear wall addition was applied in order to strengthen the frames with two floors. Two-dimensional frames, which were strengthened by an adjacent external shear wall and external shear wall with tie beams, were tested under reversed-cyclic lateral loading, respectively. The research showed that the addition of external shear walls with tie beams made a more significant contribution to a frame in terms of energy dissipation capacity. In the application by external shear walls without tie beams, there were severe cracks in the beam-column joints causing brittle failure. Kaltakci, Arslan, and Yilmaz (2011) investigated the performance of a strengthening application with an exterior reinforced concrete shear wall without tie beam. The researchers tested RC frames, each at 1/3 scale and consisting of two floors and two spans under cyclic lateral loading. The study showed that an addition of external shear walls to RC frames provided an increase in lateral strength, stiffness, and energy dissipation capacity. However, the shear walls were built on the exterior of the building; lighting and the use of balconies were affected due to adjacent shear walls without any distance between them. In addition, it was indicated that there would be some differences in the seismic behavior of the strengthened two-dimensional test frames and buildings in practice. Görgülü et al. (2012) carried out two tests on two identical two-story, 1/3 scaled RC frames under lateral cycling loading to investigate the seismic performance of strengthening RC structures with external steel shear walls. Their research presented that the proposed strengthening application improved the lateral load-bearing capacity and stiffness significantly. Ünal (2012) studied the strengthening of four 1/3 scaled specimens by column jacketing, exterior shear walls with window opening, and exterior shear wall by dividing into two pieces. The specimens were tested under reversed cyclic loading. The results presented that the addition of exterior shear walls made more contribution than strengthening of the column jacketing. Furthermore, it was observed that the increases of rigidity, load-bearing, and energy dissipation capacity of the frame strengthened by exterior shear walls with window opening were highest.

The RC frame specimens in the present study have three dimensions, as in real-life structures. Two-bay in directions, one-story, and 1/2 scaled three reinforced concrete frame specimens were tested under cyclic lateral loading. Test specimens were constructed with common deficiencies in design and material to represent the existing older structures in the building stock. The first specimen was a bare frame as

a reference. The second frame was a damaged frame, while the third frame was undamaged. The damaged and undamaged frames were strengthened by external reinforced concrete shear walls with steel tie beams. Another different point of the research was the use of steel tie beams to connect the three-dimensional frame and external shear walls. Thus, the strengthened frame specimens were investigated to obtain the strength, stiffness, energy consumption capacity, and crack formation. The structural behaviors of the frames were compared with each other to evaluate the effect of the strengthening method.

2. Material and Test Method

2.1. Test Specimens

In this experimental study, three frames and four shear walls were manufactured and tested. The test frames were designed as two-bay in both directions, one-story RC frames. Both the frames and shear walls were made of reinforced concrete with 1/2 geometric scales, as proposed by Harris and Sabnis (1999). The test frames were detailed and constructed purposely with some deficiencies commonly observed in existing buildings in many countries, such as low-quality concrete and rebar, insufficient confinement of concrete at column and beam ends, no confinement at beam-column joints, and inadequate lap splice lengths of the columns in the foundation. The ties used in the beams and columns of the test frame specimens had 90° hooks on their free ends.

All column and beam dimensions were 125/150 mm. In all columns, four outer plain bars of 8 mm diameter and two inner plain bars of 6 mm diameter were used as longitudinal reinforcement. In the beams, two 6 mm diameter plain bars on the top and three 6 mm diameter plain bars on the bottom were used as longitudinal reinforcement. In addition, one plain bar in 8 mm diameter was used as additional longitudinal reinforcement. Plain bars with a diameter of 6 mm, spaced at 60 mm, were used as ties in both the beams and columns, however, the beam-column joints were unconfined. In addition, no confinement zones were provided in the beam and column ends as a deficiency. Dimensions and reinforcement details of the test specimens are illustrated in Fig. 1.

The slab thickness was 50 mm, and the reinforcements of the slabs were 6 mm diameter in both directions. In all test specimens, material properties, geometric dimensions, and reinforcement patterns of the frames were identical. The reinforcement details of the slab and foundation of the frames are illustrated in Fig. 2 (Kucukgoncu 2018). As shown in Fig. 1, the column members are labeled “S”, the beam members are labeled “K”, and the shear wall members are labeled “SW” (Kucukgoncu 2018).

One of the identical frames was bare as a reference specimen, while the other two frames were strengthened with reinforced concrete exterior shear walls constructed to the outside of the frames. Four identical RC shear wall specimens were cast in 1/2 scale with the geometry of 875 mm length, 1500 mm height, and 125 mm thickness with an aspect ratio of 7 (‘lw/tw’, where ‘lw’ is the wall length and ‘tw’ is the wall thickness) in Fig. 1 (TEC 2007). In all cases, two walls were placed on one foundation. Sixteen steel bars with a diameter of 8 mm were used as vertical reinforcement on an RC wall. In addition, horizontal reinforcing steel bars of a shear wall consisting of two layers of 4 mm diameter bars were spaced at 75 mm. All reinforcements in the shear walls were designed in compliance with the recommendations given by the Turkish Earthquake Code (TEC 2007). Beams connecting the RC shear walls to frames were used in the IPE140 profile made of St37 steel. Deformed bars were used as anchorage in order to ensure simultaneous movement of the frame and the exterior shear wall. Holes (each 15 mm diameter) were drilled on the side face of both the beam and shear wall, starting at 70 mm from the top of the beam to the column with a 200 mm interval. After the holes were cleaned, the anchorage bars of 14 mm diameter were anchored to the pre-specified positions in the frame and shear wall, using Epoxy anchoring adhesive. An L-shaped steel plate, extending to both the beam and the column-beam joint, was welded to the anchorage bars, while a rectangular steel plate was welded to the side of the shear wall. Then, the IPE 140 steel profile tie beam, which had two

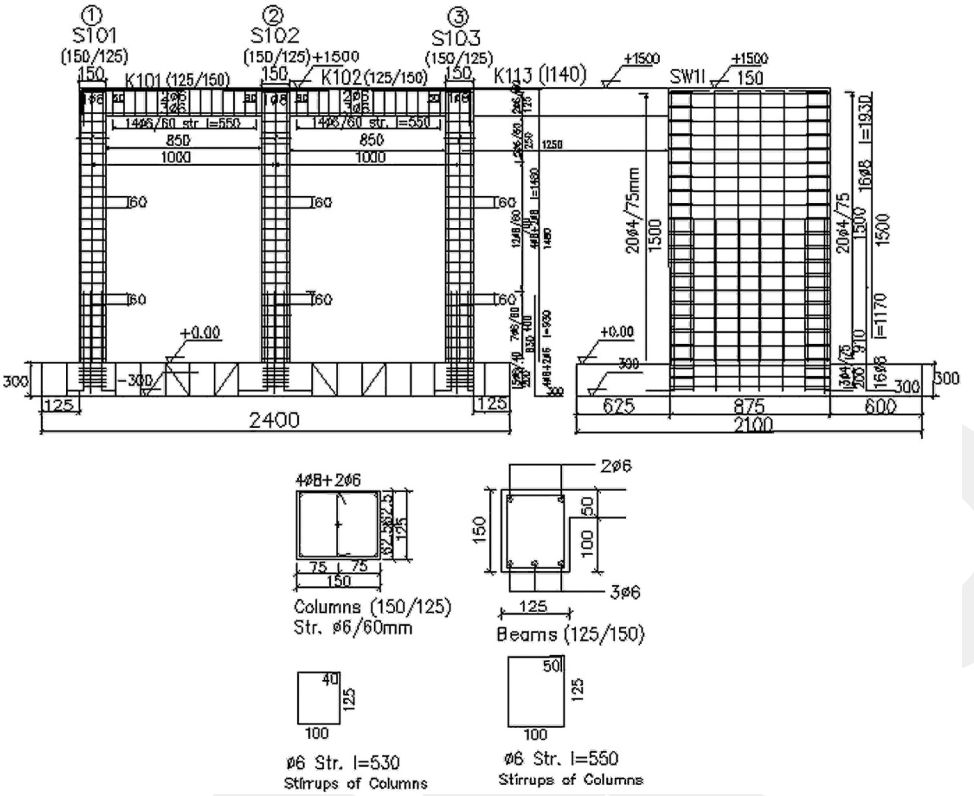

Figure 1. Dimensions and reinforcement details of the test specimens.

rows of holes drilled, was bolted to the L profile steel. Finally, the beam was placed between the frame and the shear wall and the steel beam was assembled by welding the L profile steel to the L-shaped plates.

2.2. Materials

The test frames were constructed from a low-strength concrete with a compressive strength of approximately 20 MPa to represent the concrete commonly used in existing structures, whereas relatively strong-strength concrete with a compressive strength of 35 MPa, was preferred for the exterior shear walls for strengthening according to the Turkish Earthquake Code requirements (TEC 2007). All frames and shear walls were constructed at the same time. Nine cylindrical samples were taken from each concrete grade to generate three batches. Then, they were left under the same environmental conditions with the test frames and walls in order to check the compressive strengths of the concrete materials.

Plain steel bars, which are not allowed to be used by the Turkish provision code, were used as both longitudinal and transverse reinforcements in the frames to represent existing structures. Deformed steel bars complying with regulations (TEC 2007) were used for the shear walls and foundations. The yield strengths of the steel bars were measured by a steel tension machine. The average compressive strengths of the frames and shear walls' samples obtained from the tests were 22 MPa and 35 MPa, respectively. The yield and ultimate strength of the plain bars were 325 MPa and 460 MPa, while the strengths of the deformed bars were 530 MPa and 630 MPa, respectively.

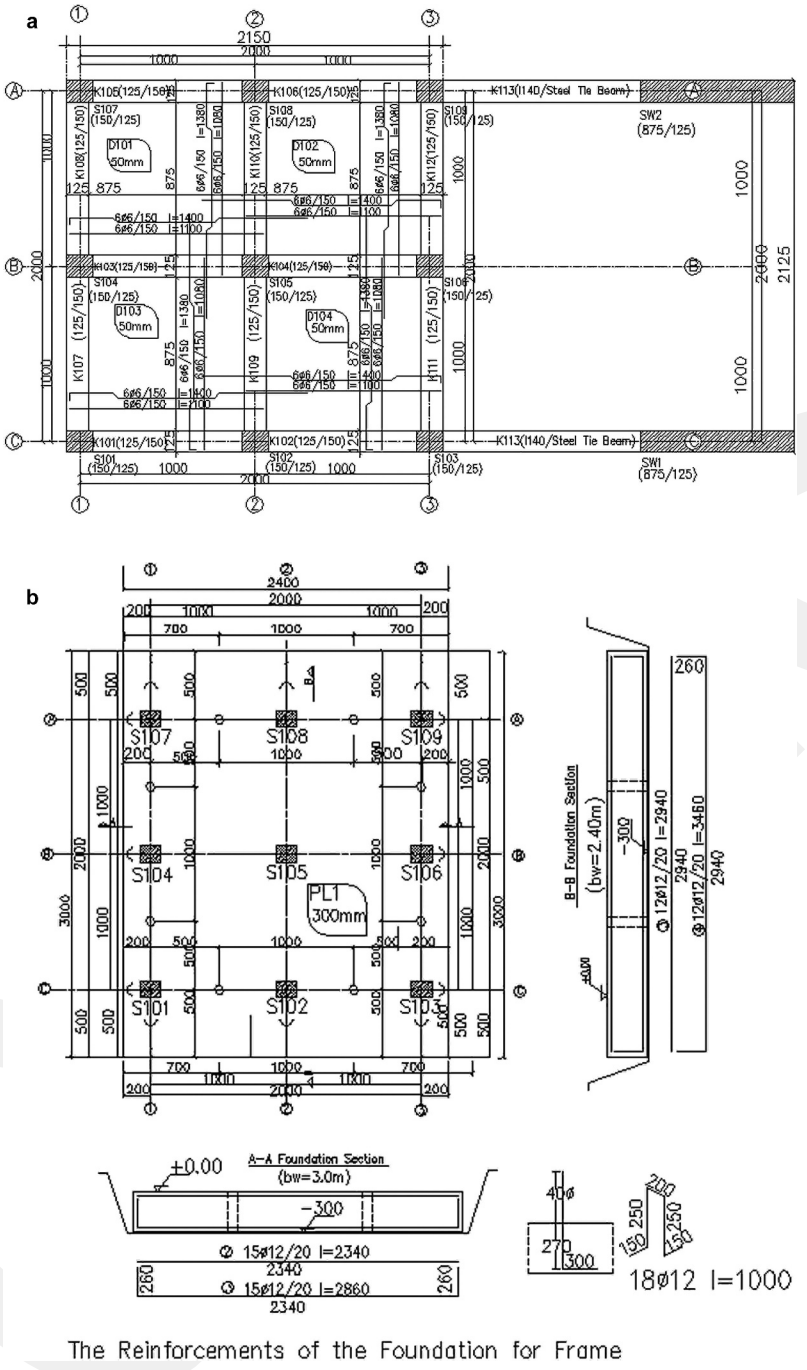

Figure 2. Reinforcement details of a) the slab b) the foundation for the frames.

2.3. Experimental Setup

A schematic view of the experimental setup and the arrangement of the devices are shown in Fig. 3. The foundations of the test specimens were anchored to the laboratory's strong floor through high strength steel bolts, in which the diameter was 36 mm, and the grade of bolts was 8.8. Specimens were

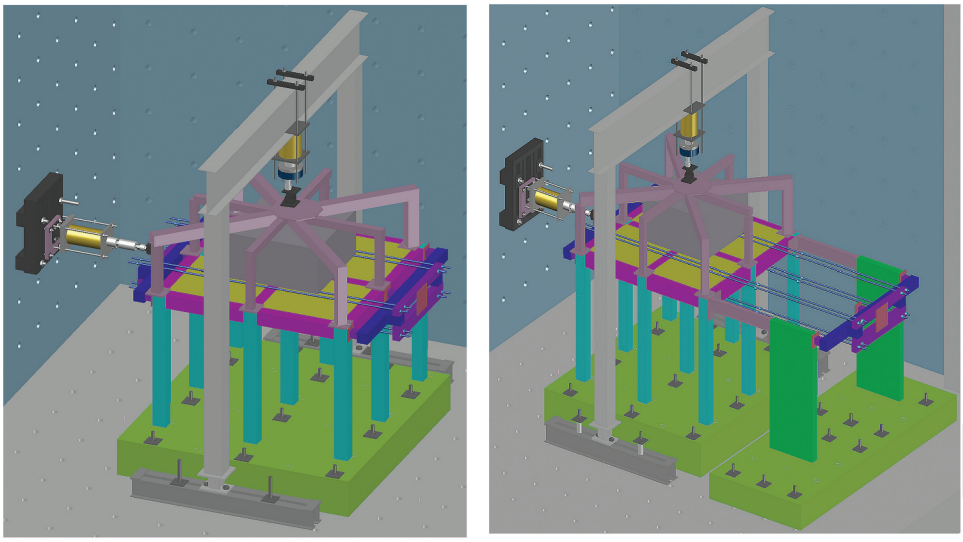

Figure 3. Schematic view of the experimental setup of a) reference frame b) strengthened frames.

tested under reversed cyclic lateral loading. A lateral load was applied to the specimens at each column-beam joint level by using a particular lateral loading setup distributing the load to each column-beam joint (to three nodes in each axis) along the loading direction. A hydraulic jack with a capacity of 600 kN in compression and 420 kN in tension connected to the rigid wall at one end and a load cell with a 500 kN compression capacity at the other end was used to apply the lateral load to specimens. Both these ends consisted of roller bearings to avoid additional effects except for axial load during lateral loading. The lateral load was applied incrementally and transmitted to the other side of the frame via transmission bolts in order to obtain the hysteretic behavior of the frame.

The axial load on the columns, approximately equal to a minimum of 10% of the column axial load capacity to ensure tensile failure in columns (N = 0.1× Ac×fck), was provided by a steel loading setup connected to the hydraulic jack with 600 kN in compression and 420 kN in tension capacity. The axial load, provided by a hydraulic jack, was distributed to each column except for the central column of the frame by using a steel vertical loading setup. Since the axial forces in the corner and edge columns are considerably smaller than the axial forces in the interior columns in practice, this setup was designed with different steel profiles to distribute the axial load to the columns in proportion to the stiffness of profiles. Thus, less axial load was provided to the corner columns compared with the other columns. In addition, a concrete block was produced to apply the required axial load to the central column. A rigid steel frame from different steel profiles constructed around the test frame was fixed to the rigid floor via anchors using two steel floor plates at one end to prevent rotation (out-of-plane deformations) due to horizontal or vertical shift. In order to enable in-plane movement during the test, the frame was fixed to the steel floor plates with roller bearings at the other end. In addition, the rigid steel frame carried the hydraulic jack providing the axial load and the load cell measuring the axial load. These can be seen in Fig. 4 and Table 1.

2.4. Instrumentation and Testing

All deformations were measured by displacement transducers using either linear variable differential transformers or potentiometers, as presented in Fig. 5. A Linear Variable Differential Transformer (LVDT) was placed on the foundation of the test frame to check whether there was any small shifting in the foundation. In order to measure the top displacement, a potentiometer measuring 300 mm (± 150 mm) was located on the middle column level in the loading direction.

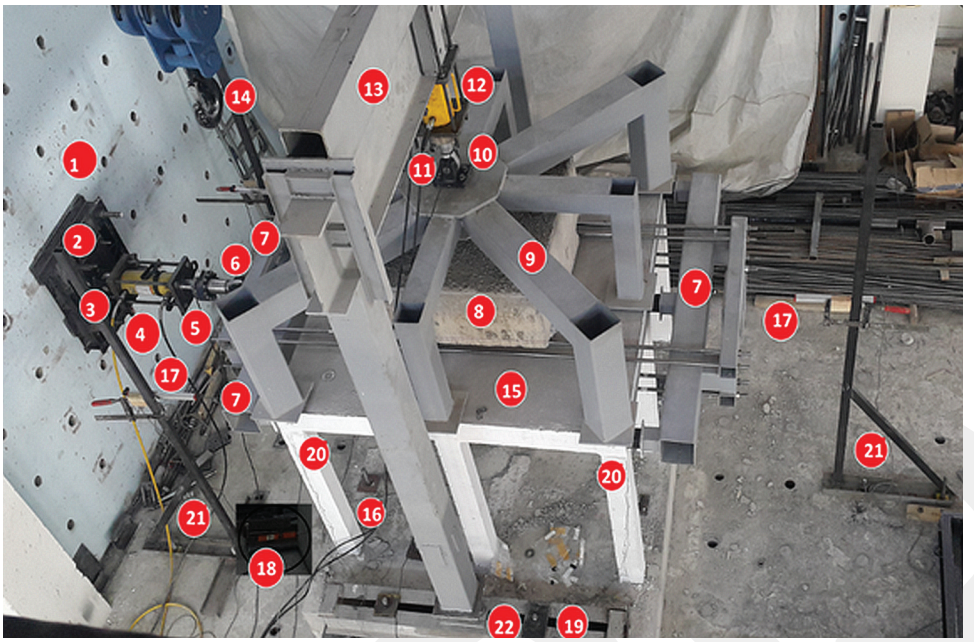

Figure 4. Experimental set up of the reference frame.

Table 1. Test devices of the setup.

No.	Device	No.	Device	No.	Device
1	Rigid wall	9	Axial loading set up	16	Anchors in the foundation
2	Steel plate	10	Roller bearing	17	Potentiometer
3	Roller bearing	11	Load cell	18	LVDT
4	Hydraulic jack	12	Hydraulic jack	19	Steel traverse
5	Load cell	13	Steel axial frame	20	Cable of strain gauge
6	Roller bearing	14	Crane	21	Trivet for measurement devices
7	Lateral loading set up	15	Reference frame	22	Roller bearing
8	Concrete block				

However, any torsional effect in the test frames was checked by two potentiometers placed on each corner columns in the push direction. Moreover, a potentiometer was located on the middle axis of the test frame and also, another potentiometer was located between the shear walls along the same loading direction in an attempt to obtain the top displacements for both the frame and shear walls.

One of three constructed specimens, a bare frame was tested at first as a reference test. Then, another identical frame was tested to make the frame damaged until pre-determined damaged levels with respect to the drift ratio. There was about 2.6% drift ratio at the end of the test, and the damage level of the frame was called 'Marked Damage Region' as stated in the Turkish Earthquake Code 2007 (TEC 2007). This damage level with a drift ratio is mentioned in the Federal Emergency Management Agency (FEMA) as either 'Life Safety (LS) Structural Performance Level' or 'Limited Safety Structural Performance Range' and defined as the continuous range of damaged states between 'Life Safety' and the 'Collapse Prevention Structural Performance Level (FEMA356 2000). Finally, damaged and undamaged frames were tested by adding exterior reinforced concrete shear walls with steel tie beams, respectively. During each test, in both push and pull half cycles, a 5 kN lateral load was applied at the beginning. In the reference frame test, the lateral load was increased by 5 kN in each cycle as far as the frame was capable of resisting higher loads, and deformation-controlled loading was applied due

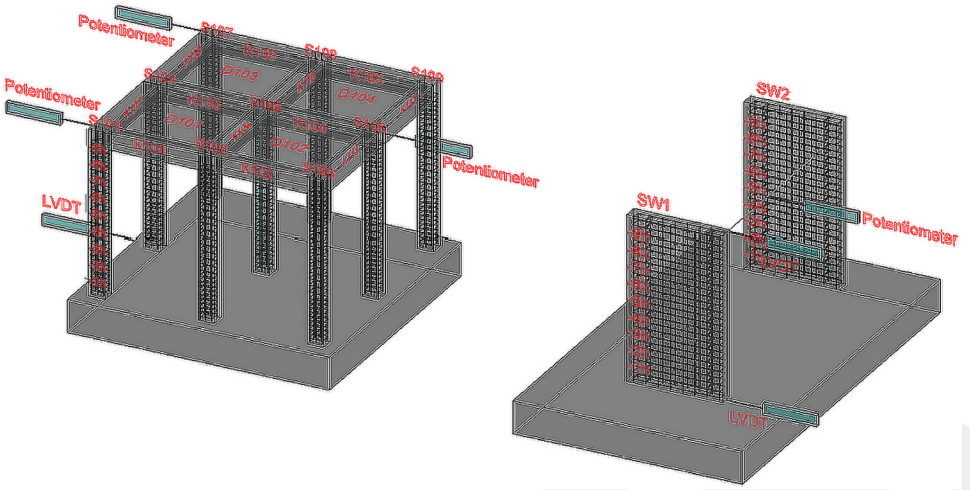

Figure 5. The arrangement of the measuring devices in the frames and shear walls.

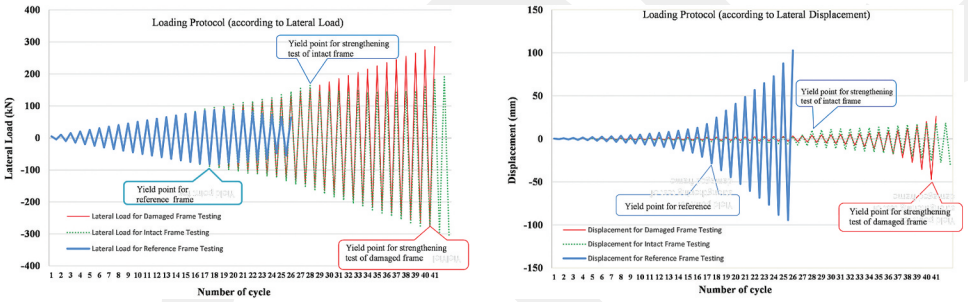

Figure 6. Loading protocols for all tests with respect to a) lateral load b) lateral displacement.

to increasing displacement values in cycles. Similarly, in the strengthening test, the lateral load was increased by 5 kN in each cycle up to the 26th cycle and then continued in 10 kN increments as load-controlled. After reaching the yielding stage, deformation-controlled loading was applied until the end of the test. Loading protocols with respect to the lateral load and lateral displacement are given in Fig. 6. Applied vertical and lateral loads were measured by two load cells. The loads were continuously monitored, and the lateral load-top displacement curve of the test frame was plotted during each test. All cracks in the frame and shear walls were marked and the failure mechanism was observed during the tests.

3. Experimental Results

3.1. Behavior of Test Specimens and Failure Mechanism

All structural components in the test frames (columns, beams, and slabs) were numbered, starting with the front axis from left to right along all axes, respectively. Additionally, each column in the frames was divided into 150 mm intervals from top to bottom in order to monitor crack formation clearly, and the intervals were represented by "h", which was denoted as column height in the loading direction (Fig. 5). The cracks that occurred in the push cycles were marked blue, whereas the cracks in the pull cycles were marked red.

For reference frame specimen RF, the first flexural cracks were recorded at the (1 h) level on the S101 column and the (8 h) level of the S104 column at a 20 kN load level. In the S105, S106, and S109 columns, the first flexural crack formations were observed in the beam-column joints. The first flexural crack in the beams occurred in K106, while the first crack was noted in the D102 slab. The first flexural-shear crack in the base-column joint was observed in the S101 column at a 65 kN load level. According to the crack monitoring during testing, the most damaged members were the columns, whereas the most damaged regions were the beam-column and the base-column joints. Buckling in reinforcements located in the base-column joint occurred. The test was completed at a 63 kN load level by a 6.85% drift due to the load level decreasing by 30%. During the following loading cycles, the intensities and widths of the cracks between the bottom of the columns and the beam-column joints increased. The reference frame at the end of the test is given in Fig. 7.

The second test was carried out to damage a frame that was identical to the reference specimen. In this test, the first flexural crack formations occurred at the (8.5 h) level of the S101 column and (1 h) and (8 h) levels of the S104 column at a 25 kN load level. During the same cycle, the first flexural crack was noted in the beam-column joints of the S107 column. The first flexural crack was observed in the column-base joint of S106 at a 35 kN load level, and it advanced towards the column in the 7^{th} cycle. In addition, the first diagonal shear crack was observed in the joint area of the S103 column in the pull loading direction, forming an X-pattern. In the K103 beam at 80 kN, the first flexural crack was observed with a width extended to 2 mm. The test was terminated at an 82 kN load level by making a 2.67% drift, which was the desired damage limit, and the roof displacement was 40 mm in order to obtain a damaged frame. During the test, the most damage occurred in the S103 column, K102 beam, and joint of S103-K102-K111.Additionally, the concrete on the right side of the K102 beam and the S103 column spilled. The reinforcements in that region became visible.

Figure 7. The reference frame at the end of the test.

In the third test, the second specimen damaged in the second test was strengthened with external shear walls. The first flexural cracks were observed at a 35 kN load level both at the (6 h) level of the S101 column and (4 h) and (7 h) levels of the S107 column. In addition, at the same load level, the first flexural-shear crack occurred in the S102 base-column joint. At a 60 kN load level, the first crack was noted in the S103-K102 beam-column joint in a flexural-shear crack pattern, while the others were noted in the S101-K101 and S102-K101 beam-column joints in an X-pattern. The first flexural crack in the beams was advanced in the K105 beam at a 100 kN load level during the 12^{th} cycle. For the external shear walls, the first shear crack occurred at the (1.5 h) level of SW1 at a 195 kN load level during the 32nd cycle. At the end of the 39^{th} cycle, the opening enlarged significantly. Then, the longitudinal reinforcements in that area ruptured when the shear cracks opened widely, and the strength of the specimen suddenly decreased. The appearance of the strengthened damaged frame at the end of the test is presented in Fig. 8.

The third specimen, which was the undamaged frame, was tested in the fourth test (Fig. 9). The first flexural cracks due to bending around all columns at the (3 h) and (6 h) levels and beam-column joint of S101-K101, S102-K102, S103-K102, S107-K105, and S108-K106 appeared at a 20 kN load level in the 4th cycle. During this cycle, the first flexural cracks occurred in the K101, K102, K105, and K106 beams, while the first flexural cracks in the base joint were noted in the S106 column. The first cracks in the slabs propagated in the D101 and D103 slabs at a 163 kN load level. In this test, the SW1 shear wall collapsed at 305 kN by reaching 21.22 mm as peak displacement because of the visible opening between the bottom of the SW1 shear wall and the base joint, starting from the right corner of the shear wall to the front face.

For the RC frame specimens, the formation of the first flexural cracks in the columns occurred in the first and fourth tests in earlier cycles compared to the other experiments. The first horizontal flexural crack formation in the base-column joint observed in the strengthening test of the undamaged frame was the earliest, while it was the latest in the reference test. The first flexural-shear crack in the beam-column joints appeared in the strengthening test of the undamaged frame during the earliest cycles, whereas in the latest cycles in the strengthening test of the damaged frame. The intensity and the width of flexural cracks increased with incremental load significantly. Although the shear cracks in the columns propagated from the beam-column and base-column joints to the mid-sections of the

Figure 8. The appearance of the strengthened damaged frame at the end of the third test.

Figure 9. The strengthened system in the 40th push cycle in the fourth test.

column by increasing horizontal load, no crack formations in most of the columns were observed between the (3 h-6 h) level on the pull faces and (4 h-6 h) level on the push faces during all testing. Moreover, the ratio of non-cracked areas in the middle section of the column increased, especially in the undamaged frame because of the addition of the shear walls to the structural system. The first flexural crack in the beams developed in earlier cycles with the addition of the shear walls to the system, but it was observed that the crack intensity decreased by strengthening the frames. Since the frame specimens that were defective and weak in terms of earthquake resistance were investigated, the first flexural cracks in the beams occurred before the yield load due to the mechanism and plastic hinge during all tests. Although most of the crack patterns observed in the columns, beams, and joints were flexural cracks, some shear cracks appeared in column members and column-beam joints. However, no torsional crack was observed in any element during all the tests. The most damaged columns of the reference frame at the end of the reference, strengthened damaged and undamaged tests are illustrated in Fig. 10. The flexural cracks occurring in beams due to tensile forces and bending moments generally were observed in the lower and upper faces of the beams in the areas closest to the supports. Compression failure occurred because of crushing in the concrete of the base-column joints. Additionally, buckling in the longitudinal reinforcements of the columns was observed, and a plastic hinge appeared at the bottom of the column. Furthermore, significant damage appeared in the reference frame before and after the maximum load, but no significant damage and cracks occurred in the strengthened frames at the maximum load level. As shown in Fig. 10, the crack intensity and the width in the strengthened frames decreased due to the addition of shear walls.

4. Discussion of Test Results

4.1. Hysteric Behavior

Lateral load and displacement values obtained from the load cells, LVDTs, and potentiometers during all tests were plotted as hysteretic curves. These curves, giving information about the seismic performances of the test specimens, are presented in Fig. 11. The successive hysteresis loops obtaining during the loading and unloading formed the hysteresis curve. The upward slope area in the first region of the hysteretic behavior represents the linear behavior of the specimen. During the cycles in that region, the capillary cracks occurred as opening and closing. As the cycles progressed, existing crack propagation occurred as well as new cracks formation, depending on the behavior of the structure. There was an upward slope in the linear region, while a descending slope in the nonlinear

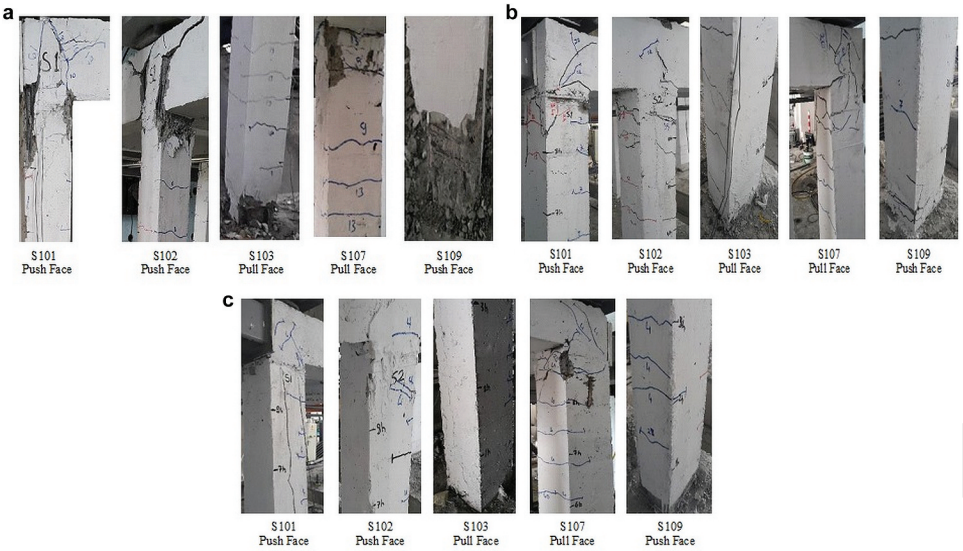

Figure 10. (a) Damage appeared in some columns of the reference frame at the end of the test. (b) Damage appeared in some columns of the strengthened damaged frame at the end of the test. (c) Damage appeared in some columns of the strengthened undamaged frame at the end of the test.

region in the hysteresis loops. The strength, stiffness degradation, ductility, and energy dissipation capacity of the specimens were calculated from the hysteresis curves. These curves represent the behavior of the reference and strengthened frames during cycling loading (Clough 1966; Takeda, Sozen, and Nielsen 1970).

As seen in Fig. 11, the strength of the strengthened damaged frame increased by 2.71 times, while the displacement of the frame decreased by 71.86% approximately due to the external shear walls. Compared to the hysteresis curves of the undamaged frame strengthened by external shear walls with the reference frame, the strength of the strengthened frame increased 2.41 times. However, its displacement decreased by 79.41%. As a result, the displacement of the strengthened undamaged frame by external shear walls was the lowest, whereas its strength was the highest of all test frames. During all testing, the load was monitored until the nominal yield load of the system and after the yielding, the displacement was monitored. The lateral load values were higher than the yield load during the displacement checked for all specimens. The reason is the loading speed during the test and the monolithic structure of the reinforced concrete bearing system. In accordance with the principle of the redistribution of loads in the reinforced concrete structural elements because of the monolithic structure of concrete, the lateral loads in some concrete fibers of the column that reached the collapse limit were carried by the fibers in the other columns in the subsequent cycles. The yield loads and corresponding displacements of all test frames are given in Table 2.

In the carried out experiments, the lowest yield loads were obtained from the reference frame, the strengthened undamaged frame, and the strengthened damaged frame, respectively. Thus, the yield loads of the systems increased by adding external shear walls to the frames. It was observed that the damaged frame reached a higher yield load than the undamaged frame. However, it was considered that the strengthened undamaged frame reached its yield load point during only push cycles because the lateral load did not increase significantly in later push cycles. Since there was no opening in the slabs, the hysteresis curves obtained from the other experiments except for the undamaged frame test, were symmetrical due to diaphragm effects. In addition, there are some differences in the behavior of the undamaged strengthened frame in the pull and push cycles in Fig. 11. Since there was no crack in the undamaged strengthened frame, the initial stiffness became effective in the undamaged strengthening test. However, the loss of rigidity occurred due to some cracks in the damaged strengthened frame. Thus, there was no difference in both push and pull cycles due to the loss of

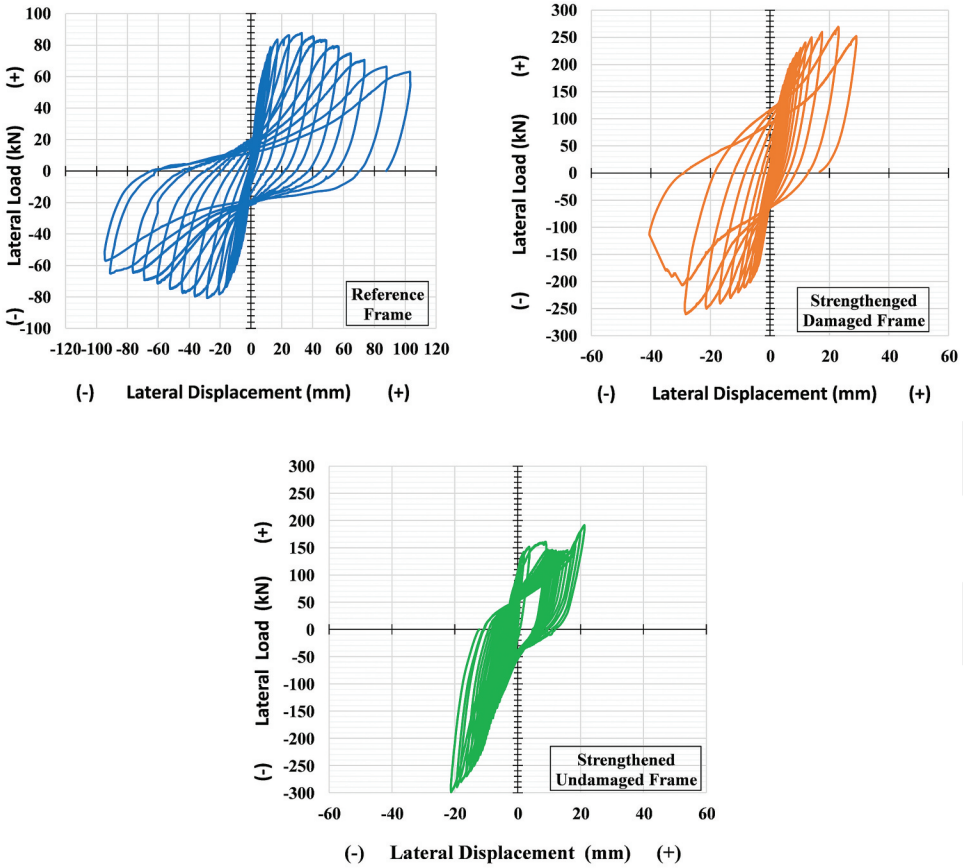

Figure 11. Lateral load–lateral displacement responses of the frame specimens.

Table 2. The yield load and displacement of the test frames.

Specimen	Test Number	Cycle Number	Loading Direction	Yield Load (kN)	Displacement (mm)
Reference Frame	1	17	Pull	82	27.96
Strengthened Damaged Frame	3	41	Pull	207	29.04
Strengthened Undamaged Frame	4	28	Push	164	9.11

rigidity in this test. Additionally, the distance of strengthening the external shear wall to the loading system caused differences in the pull and push behavior. By comparing the displacements corresponding to the yield load point in all experiments except the strengthening of the undamaged frame test, the displacement capacity of the reinforced concrete structural systems decreased by the addition of shear walls. As compared with the displacements corresponding to the maximum lateral load in all the experiments, there was a decrease in the displacement capacities of the frames due to the shear walls. Therefore, the evaluations in this part were carried out according to the maximum lateral load instead of the yield loads of the frame specimens.

4.2. Strength Envelopes

The strength envelope curves of the test frames were obtained from the peak lateral load and the top displacements corresponding to these points for each cycle in every pull and push stage. The test results are summarized and presented in Table 3. This table was prepared for illustrating the effect of

Table 3. The lateral load bearing capacity of the test specimens.

Test Specimen	Maximum Lateral Load/Displacement		The Ratio of Maximum Lateral Load
	Lateral Load (kN)	(δ/H)	
Reference Frame	87.75	0.02195	1
Strengthened Damaged Frame	270	0.01528	3.07
Strengthened Undamaged Frame	300	0.01412	3.41

strengthening with the external shear walls in the ultimate lateral load, displacement, and drift ratio. In addition, the strength envelope curves obtained from all the frame specimens are shown in Fig. 12.

The envelopes obtained during the push cycles were plotted in blue, while obtained from the pull cycles were shown as red. The maximum lateral load capacity in the push cycle of the reference, strengthened damaged, and strengthened undamaged frames were 87.75 kN, 269.55 kN, and 191.40 kN, respectively. The damaged and undamaged frames strengthened with external shear walls had 207% and 118% more maximum lateral load than the reference frame, respectively. The maximum lateral load value with the pull cycle for the reference frame was 80.66 kN. However, these values were measured as 265 kN for the second test specimen and 300 kN for the third test specimen. In conclusion, the lateral load-bearing capacity increased in the strengthening of the damaged frame system. A larger increase was obtained for the undamaged frame strengthened by the external shear walls. In the push cycles, the top displacements of the reference, strengthened damaged, and

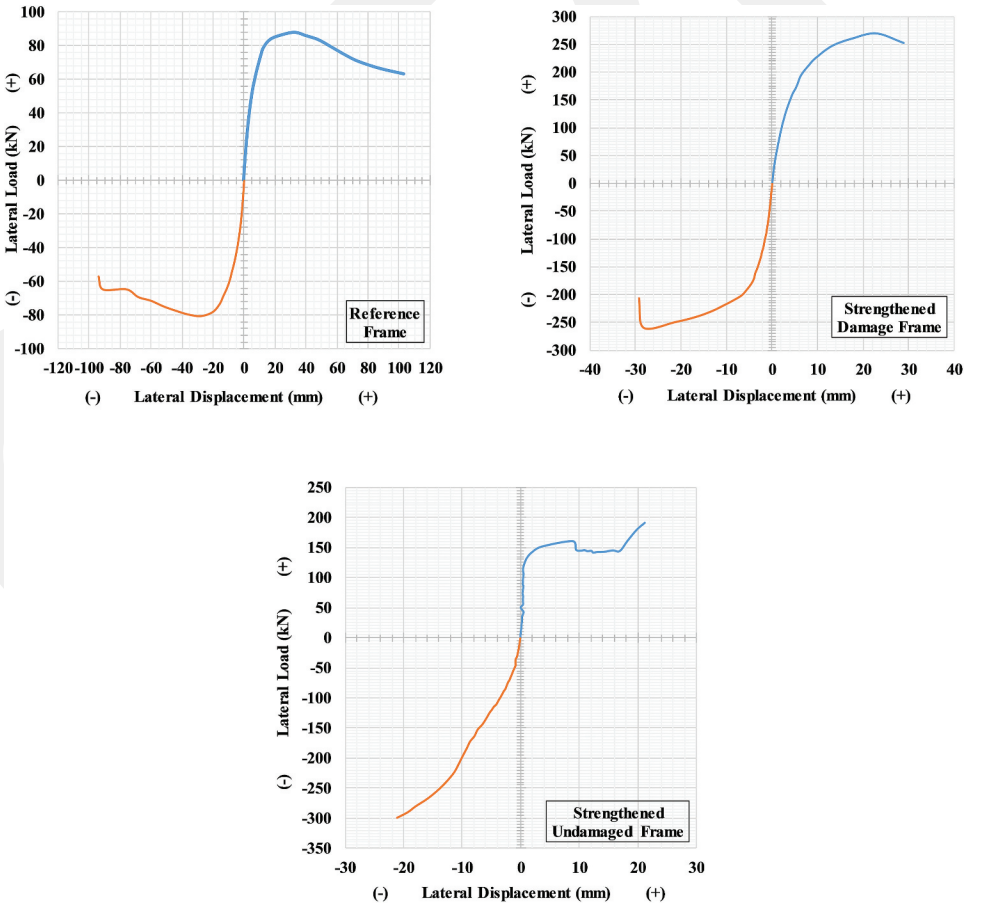

Figure 12. The strength envelope curves of the frame specimen.

strengthened undamaged frames were measured as 103 mm, 28.98 mm, and 21.21 mm, respectively. By adding the external shear walls to the frames for strengthening, the degradation in the displacement capacity of the damaged frame was 71.86%, whereas it was 79.41% for the undamaged frame in the push cycles. Additionally, the top displacements in the pull cycles were 94.12 mm in the reference specimen, 29.24 mm in the damaged frame, and 21.18 mm in the undamaged frame. It was observed that the deformation capacities of the second and third specimens at 68.93% and 77.46% dropped in the pull cycles, respectively, due to the external shear walls. Table 3 presents the lateral load-bearing capacity of the frame specimens obtained during the tests.

The drift ratios corresponding to the maximum lateral load for the reference frame, the damaged and undamaged frames strengthened with external shear walls, are given in Table 3. The experiment with the top displacement reaching the highest value was the reference frame test due to the ductile behavior of the frame. Addition of the external shear walls for the purpose of strengthening defective frames resulted in both the strength and the stiffness increase significantly in not only the frames but also in the systems.

4.3. Stiffness Degradation and Displacement Ductility

In structural engineering, the term 'stiffness', referring to the rigidity of a structural element, is defined as a measure of being able to resist deformation or deflection by the structural element under an applied force. As the stiffness of structural bearing systems increases, the lateral force required for deformation of the system must be increased. It is known that degradation in stiffness of a specimen occurs due to the formation of plastic hinges under lateral loads in the experimental research. For comparison of the stiffness values of the test frames, stiffness was investigated. The stiffness of a test specimen was determined by using the slope of the load-displacement graph for each pull and push cycle. Hence, the lateral load values obtained from the lateral load-displacement curve in each cycle are represented as F_1 and F_2, while the horizontal displacement values corresponding to these load values are referred to as δ_1 and δ_2. Then the stiffness value (ϕ) of that cycle was calculated using Eq. (1) as follows;

$$\text{Stiffness}(\phi) = \frac{(|F1| + |F1|)}{(|\delta 1| + |\delta 2|)} \tag{1}$$

Stiffness degradation curves were obtained by plotting the calculated stiffness values versus the ratio of the peak displacement/story height (δ/H) graphically. The stiffness degradation curves based on the δ/H ratio instead of the number of cycles for better comparison of the test results are shown in Fig. 13.

As seen from the graphs given above, the initial stiffness of the reference frame was measured as 15.92 kN/mm, and then the stiffness decreased rapidly in the later cycles. Particularly, it was observed that the degradation in the stiffness slowed after the values of δ/H reached 0.02 for the reference frame. Furthermore, the initial stiffness of the damaged frame, strengthened with the external shear walls, was calculated as 102.35 kN/mm, whereas the initial stiffness of the strengthened undamaged frame was calculated as 105.71 kN/mm. Similarly, the decreases in the stiffness of the strengthened specimens were observed in the later cycles. It was seen that the decreases in the stiffness slowed after the value of δ/H reached 0.009 for the damaged frame, while it reached 0.005 for the undamaged frame. The stiffness values and drift ratios (δ/H) at critical points such as initial, maximum lateral loading, and failure are given in Table 4.

According to Table 4, the strengthened damaged and undamaged frames had higher initial and maximum lateral loading stiffness values than the reference frame did. The stiffness degradations of all specimens are given comparatively in Fig. 14.

Figure 14 also shows that all the stiffness values of the strengthened frames were higher than the stiffness of the reference frame. Thus, adding shear walls to the frames for strengthening considerably

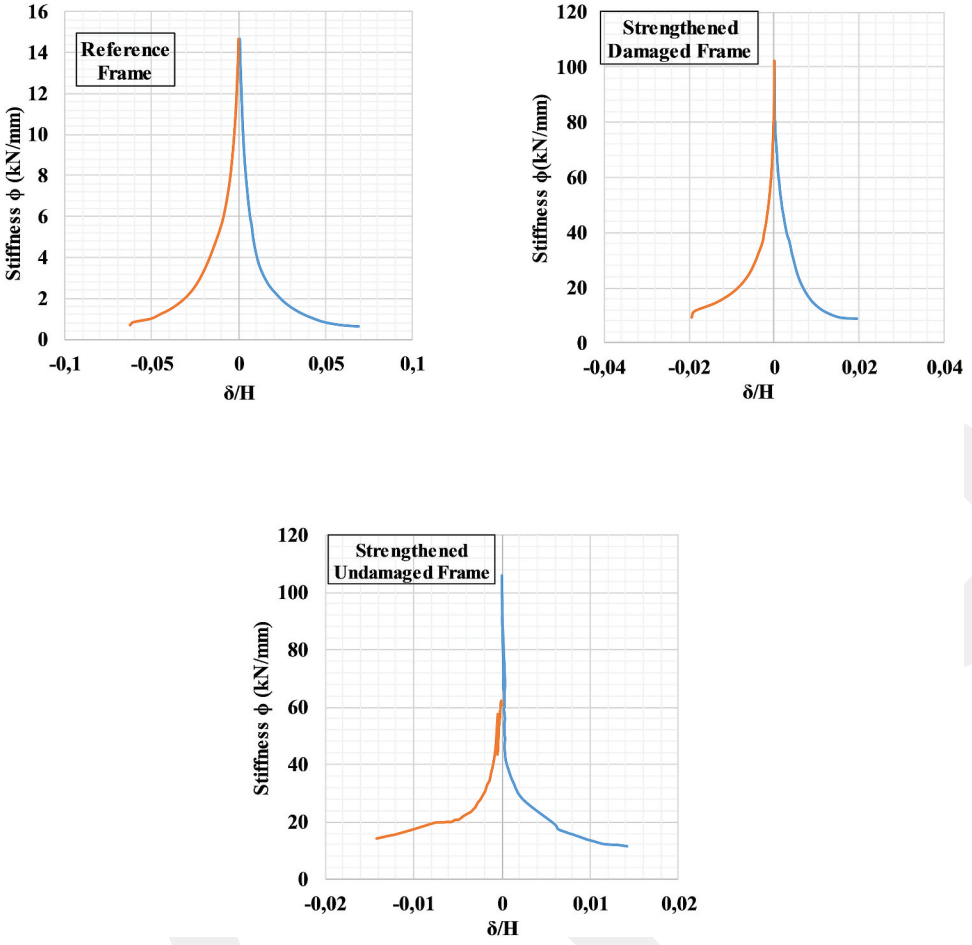

Figure 13. Stiffness degradation curves of the test frames.

Table 4. The stiffness of frames in selected important stages.

	Stiffness (kN/mm)			(δ/H)			
Test Specimen	First Cycle	Max. Load	Last Cycle	Max. Load	Last Cycle	The Ratio of Initial Stiffness	The Ratio of Stiffness at Maximum Load
Reference Frame	15.93	2.14	0.61	0.022	0.069	1	1
Strengthened Damaged Frame	102.36	9.13	8.71	0.015	0.019	6.43	4.27
Strengthened Undamaged Frame	105.71	11.57	11.57	0.014	0.014	6.64	5.4

increased the rigidity of both the frames and the system. Additionally, it was observed that the stiffness of the undamaged frame was higher than the stiffness of the damaged frame by comparing the strengthening tests. The reason was that the strength and the rigidity of the undamaged frame were higher than the damaged frame and the stiffness values of the shear walls added to the frame had similar behaviors to the frame.

Ductility is defined as the energy dissipation capacity of a structural bearing system under applied loads, and it has a great influence, especially on structural systems under earthquake ground motions. The displacement ductility of a specimen was calculated by the ratio of the maximum displacement, which the structural system was able to reach the yield displacement.

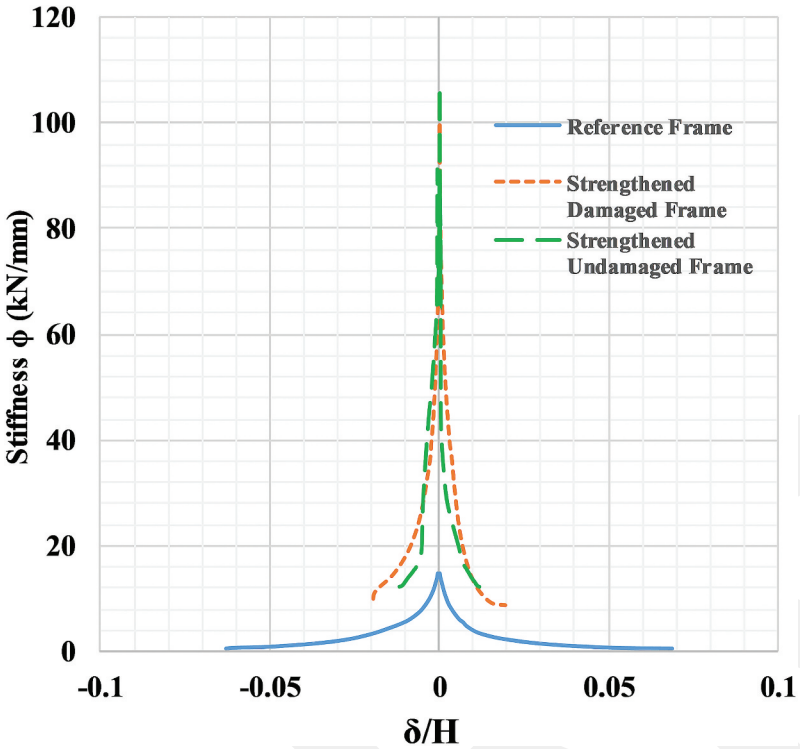

Figure 14. The comparison of the stiffness degradations curves of all specimens.

A graphical method was used to reach the displacement ductility values of the frames with the help of envelope curves obtained from the hysteresis curves. After the envelope curve was drawn, the maximum lateral load point (F_{max}) and the corresponding displacement point (Δ), were marked in the forward and backward cycles. Then, the displacement point where the maximum load decreased by 25% was marked as Δ_1 on the envelope curve. Both the coordinates of the peak point of the cycle (F_{max}, Δ) and the peak point of the cycle before two cycles ($F_{max\text{-}2}$, $\Delta_{max\text{-}2}$) were marked on the envelope curve. Moreover, the displacement value corresponding to the intersection point of the curves where a 25% decrease in lateral load with the tangent drawn to the envelope curve was obtained as Δ_2. In addition to the displacement point where the maximum lateral load (F_u) decreased by 20%, was obtained and named as Δ_{max}. Finally, the yield displacement value Δ_y was determined using these load and displacement points on the envelope curve graphically (Fig. 15). Thus, the displacement ductility values of the test specimens were calculated for both the push and pull cycles by using Eq. (2) as following (Dirikgil and Atas 2019);

$$\mu = \frac{\Delta max}{\Delta y} \tag{2}$$

The maximum displacement, yield displacement, and displacement ductility values of the test frames are given in Table 5. In addition, the mean displacement ductility values were calculated by using the values of the push and pull cycles for better comparison. In comparison with all frames, the highest displacement ductility value was obtained from the reference frame. Additionally, it was observed that

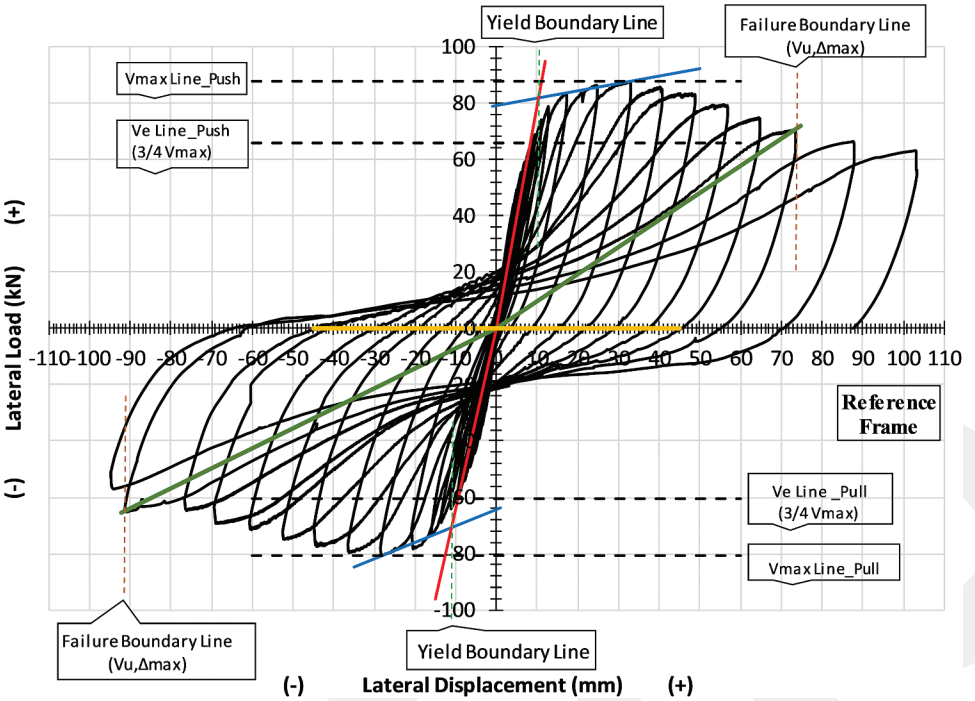

Figure 15. The scheme of the displacement ductility calculation diagram for the reference test specimens.

Table 5. The displacement ductility coefficient of the test specimens.

Test Specimen	Push Direction			Pull Direction				
	Δ_{max}	Δy	μ	Δ_{max}	Δy	μ	Δy_{avg}	μ_{avg}
Reference Frame	73.45	10.35	7.1	91.26	11.04	8.26	10.7	7.68
Strengthened Damaged Frame	7.97	8.19	1.17	8.58	6.5	1.32	7.34	1.25
Strengthened Undamaged Frame	7.74	7.18	1.09	5.73	5.62	1.02	6.4	1.06

the displacement ductility of the damaged frame was higher than the displacement ductility of the undamaged frame.

4.4. Energy Dissipation

The energy dissipation capacity is an important indicator of evaluating the earthquake behavior of structural systems. However, structural bearing systems under reversed cyclic loading consume part of the energy by deformation because of their inelastic behaviors. In this method, the energy consumption is proportional to the displacement capacity. Therefore, the amount of energy consumed by the test frame was calculated at the end of each experiment. Energy dissipation capacity depends not only on the properties of the structural member, such as reinforcement ratio, arrangement of reinforcing bars, material properties, cross-section, and size of the member, but also strongly depends on the experimental parameters, such as loading history, support conditions, peak load level, yield displacement, axial load level, and number of cycles (Park and Eom 2004).

For each specimen, the amount of dissipated energy was obtained by calculating and adding the areas under the hysteretic lateral load–displacement curves for each cycle. Firstly, the areas under the lateral load-displacement curve were obtained from forward loading and then backward loading was calculated. After that, the total amount of dissipated energy for only one cycle was computed by adding

these two areas. Finally, the total amount of energy consumed by the frame was reached by adding the areas computed in each cycle. The amount of energy stored per cycle, the recoverable elastic energy per cycle, and the cumulative energy were calculated at the end of each testing. They are presented comparatively in Fig. 16. The energy consumption graphs depending upon the δ/H ratio for a better comparison of the test results are given in Fig. 17.

The amount of energy dissipation of the reference frame was calculated from Figs. 16 and Figure 17 as 45195 kN.mm, while the same parameter was higher by 148.22% at 66989 kN.mm for the damaged frame strengthened by external shear walls. On the contrary, it was observed that the result of the undamaged frame strengthened by external shear walls was close to the reference frame, even if it was lower by 11.81% at 40420 kN.mm. It was supposed that the highest amount of energy consumption would be observed in the reference frame because of its ductile behavior, but the strengthened

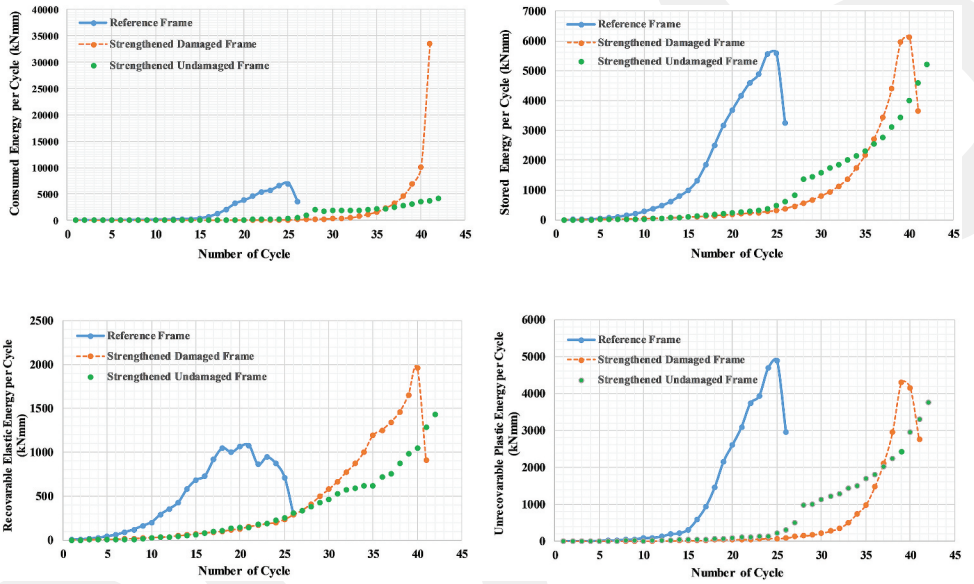

Figure 16. The energy values of the test specimens.

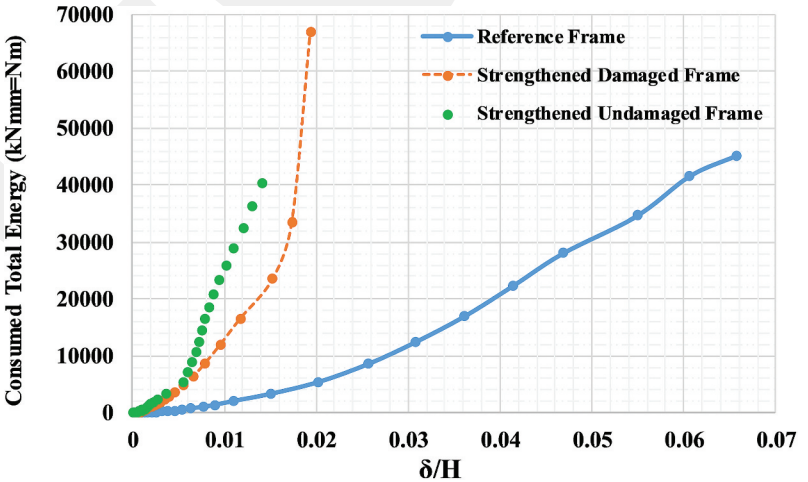

Figure 17. The consumed total energy values of the test specimens.

damaged frame system had the highest energy dissipation capacity according to the experimental results. One of the reasons why the energy consumption of the damaged frame system was higher than the other systems was the cracks opening and closing during the cycles and thus consuming energy. Another reason was that the decreasing rigidity of the damaged frame, due to some damage and cracks, consumed energy with the help of the external shear walls and especially the steel tie beams connecting to the shear walls and the frame. This case was not observed in the strengthened undamaged frame because of its high rigidity. In addition, the displacement capacity of the undamaged frame strengthened by the external shear walls with steel tie beams was lower than both the reference and damaged frame systems.

Cumulative total energy consumption values were calculated by successive summation of energy consumed in each cycle, and the graphs of the cumulative total energy consumption for all experiments are presented comparatively in Fig. 18. According to the experimental results, the amounts of energy consumption from high to low value for damaged, reference, and undamaged frame systems are shown, respectively. The results of cumulative total energy consumption were similar to the total amount of energy consumed as expected, and the increase in lateral load after a point in the push cycles in the strengthened undamaged frame experiment was considered as another reason for that case.

The energy data values of the test frames are shown in Table 6. There are no significant differences between the amounts of the stored energy of the reference frame and the strengthened undamaged frame. By considering recoverable elastic and unrecoverable plastic energy, the recoverable elastic energy value of the strengthened undamaged frame was higher, while its unrecoverable plastic energy was lower than the reference frame's. Despite the fact that the amounts of the stored and unrecoverable plastic energy of the strengthened damaged frame were lower than the other frames, the amounts of consumed and recoverable elastic energy of that frame were higher.

Since the energy consumed at the end of the experiment was also related to the number of cycles, one of the more suitable comparison parameters was considered the energy consumed in the case of

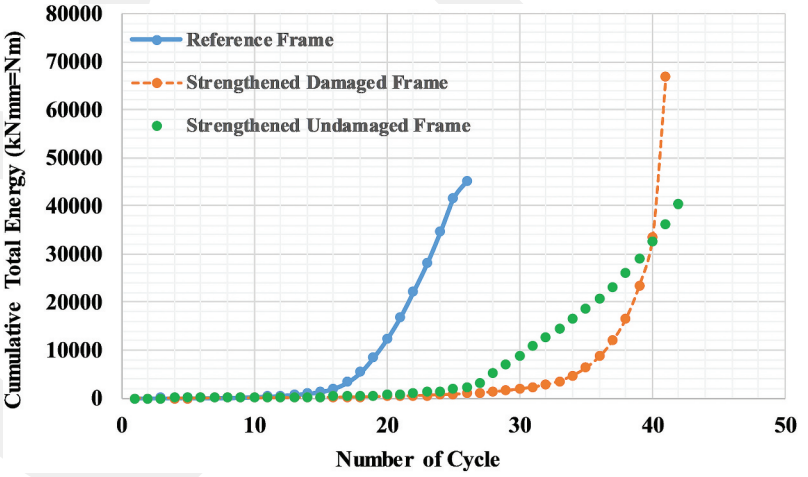

Figure 18. The cumulative total energy consumptions of all test frames.

Table 6. The energy data calculated for frame specimens.

Test Specimen	Consumed Energy Et (kN.mm)	Stored Energy Ed (kN.mm)	Recoverable Elastic Energy (kN.mm)	Unrecoverable Plastic Energy (kN.mm)
Reference Frame	45195.109	44701.599	12539.494	32162.105
Strengthened Damaged Frame	66988.995	38922.175	16965.418	21956.758
Strengthened Undamaged Frame	40419.928	44505.676	13730.55	30775.126

Table 7. The energy dissipation capacity of the test frames.

	Consumed Energy (kN.mm)		The Ratio of Consumed Energy	
Specimen	Maximum Load	End of Test	Maximum Load	End of Test
Reference Frame	8600.54	45195.11	1	1
Strengthened Damaged Frame	33494.57	66989	3.89	1.48
Strengthened Undamaged Frame	40419.93	40419.93	4.7	0.89

maximum lateral load. According to the amount of the dissipation energy in the case of maximum lateral load given in Table 7, the highest amounts of the dissipation energy are noted in the strengthened undamaged and damaged frame systems, respectively. In conclusion, reinforced concrete frames strengthened by reinforced concrete external shear walls with steel tie beams consumed more energy under cyclic loading. Additionally, it was expected that in high-rise structural frame systems, an increase in the number of frame joints and the effect of the tie beam would increase energy consumption.

5. Conclusion

In this study, an external shear wall strengthening method was investigated as an alternative to the traditional strengthening methods, which require users to vacate their buildings and cause additional heavy costs due to the length of construction time and difficulties in the application. For this purpose, 1/2 scale, one-story, three-dimensional three reinforced concrete frames, containing common deficiencies to represent existing older structures were tested under cyclic lateral loading. External shear walls with steel tie beams were added to the frames. The following conclusions were drawn in light of this experimental study.

- According to the test results, the damaged and undamaged frames strengthened with external shear walls had 3.41 times and 3.07 times more maximum lateral load than the reference frame. Thus, the maximum lateral load capacities of the frames increased due to the external shear walls. Additionally, the yield load obtained from the strengthened damaged frame was 2.52 times higher than obtained from the reference frame. However, the displacements corresponding to the maximum lateral load for strengthened frames were lower than the reference frame (Table 3). By strengthening the reinforced concrete structural systems using external shear walls, the system is enabled to reach a higher yield load, and less displacement under maximum lateral load is allowed.
- The initial and maximum lateral loading stiffness values calculated from the strengthened undamaged frame increased 6.64 times and 5.4 times than the reference frame (Table 4). In addition, all stiffness values of the strengthened frames were higher than the stiffness of the reference frame (Fig. 14). Since stiffness refers to a measure of being able to resist deformation by the structural element under an applied force, strengthened frames had less displacement under higher lateral load. Thus, the proposed strengthening application provided an increase in the stiffness of strengthened reinforced concrete frames.
- Based on the test results, the damaged frame strengthened by external shear walls consumed higher energy by 148.22% than the reference frame (Fig. 17). The amounts of the consumed energy in the case of maximum lateral load calculated from the strengthened undamaged and damaged frame systems were 4.17 and 3.89 times higher than the reference frame, respectively (Table 7). Hence, the addition of external shear walls to the reinforced concrete frame for strengthening increased the energy consumption of the structural system.

- When the reference and the strengthened frames were on the same displacement level, both stiffness and energy consumption increased in the strengthened frames because of the external shear walls. The crack formation in the strengthening frames appeared during the later cycles. Since the crack intensity and the size of the width decreased due to the addition of shear walls, damage level and density in the structural system decreased.

According to the results obtained from the experimental study, strengthening of the reinforced concrete structural system by the external shear walls with steel tie beams contributed to the strength, stiffness, and energy consumption capacity significantly. The distinctness and an original result of the research are that if there is no other defect in the structure that requires a need for other strengthening methods, this method is sufficient in order to strengthen in an effective, economical, and practical way. At this point, it should be noted that earthquakes induce lateral forces in two perpendicular planar directions. Although the external wall system is composed of walls in one horizontal direction in the study, it is suggested in light of the study results that strengthening by external shear wall application in buildings deemed necessary could be applied in two directions. Nevertheless, this type of application might be cumbersome due to the costs and workmanship.

In practice, it is suggested that the strengthening method in the study is both practical and effective to provide rapid strengthening in low to medium-rise buildings, house constructions, and public buildings, like schools and hospitals that are continuously utilized and cannot be emptied during application. Thus, the external shear wall strengthening method prevents additional heavy costs, such as rent, removal expenses, and loss of time. Since the foundations of the shear walls may need deep foundations instead of shallow foundations to resist overturning moments, this strengthening application has some restrictions for high-rise buildings. Additionally, the external shear walls should be extended throughout the entire height of the structure to provide continuity of the lateral load resisting system. Due to these reasons, the proposed strengthening method might seem impractical and costly, especially in high-rise buildings. However, the strengthening method by external shear walls, which might be applied more practically and efficiently, might be developed for high-rise buildings in further studies by using the research results.

Acknowledgments

This study was conducted in the Structural Mechanics Laboratory at Erciyes University and supported financially by Erciyes University, Scientific Research Project Funding (ERU-BAP), under Project number: FDK-2017-7722. The authors would like to thank them for their support.

Funding

This work was supported by the Erciyes University, Scientific Research Project Funding [ERU-BAP, Project Number: FDK-2017-7722].

ORCID

Hurmet Kucukgoncu http://orcid.org/0000-0001-5148-8753
Fatih Altun http://orcid.org/0000-0002-6378-9964

References

Altin, S., Ö. Anil, M. E. Kara, and M. Kaya. 2008. An experimental study on strengthening of masonry infilled RC frames using diagonal CFRP strips. *Composites Part B-Engineering* 39 (4): 680–93. doi: 10.1016/j.compositesb.2007.06.001.

Amjad, J., A. M. Aref, and W. Y. Jung. 2003. Energy-dissipating polymer matrix composite-infill wall system for seismic retrofitting. *Journal of Structural Engineering* 129 (4): 440–48. doi: 10.1061/(ASCE)0733-9445(2003)129:4(440).

Anil, O., S. Altin, and M. E. Kara. 2008. Strengthening of RC non ductile frames with RC infills: An experimental study. *Cement and Concrete Composites* 30 (7): 612–21. doi: 10.1016/j.cemconcomp.2007.07.003.
Aoyama, H., D. Kato, H. Katsumata, and Y. Hosokawa. 1984. Strength and behavior of post cast shear walls for strengthening of existing R/C buildings. Proceeding of the 8th World Conference on Earthquake Engineering, 485–92, San Francisco, CA.
Badoux, M., and J. O. Jirsa. 1990. Steel bracing of RC frames for seismic retrofitting. *Journal of Structural Engineering* 116 (1): 55–74. doi: 10.1061/(ASCE)0733-9445(1990)116:1(55).
Bal, İ. E., H. Crowley, R. Pinho, and F. G. Gülay. 2008. Detailed assessment of structural characteristics of Turkish RC building stock for loss assessment models. *Soil Dynamics of Earthquake Engineering* 28 (10–11): 914–32. doi: 10.1016/j.soildyn.2007.10.005.
Bousias, S., A. L. Spathis, and M. N. Fardis. 2007. Seismic retrofitting of columns with lap spliced smooth bars through FRP or concrete jackets. *Journal of Earthquake Engineering* 11 (5): 653–74. doi: 10.1080/13632460601125714.
Calvi, G. M. 2013. Choices and criteria for seismic strengthening. *Journal of Earthquake Engineering* 17 (6): 769–802. doi: 10.1080/13632469.2013.781556.
Canbay, E., U. Ersoy, and G. Ozcebe. 2003. Contribution of reinforced concrete infills to seismic behavior of structural system. *ACI Structural Journal* 100 (5): 637–43.
Çırak, İ. F., H. Kaplan, S. Yılmaz, Ö. Ç. Değirmenci, and N. Çetinkaya. 2015. A model for shear behavior of anchors in external shear walled frames. *Research on Engineering Structures and Materials* 1 (2): 53–71. doi: 10.17515/resm2015.05st0211.
Clough, W. 1966. *Effect of stiffness degradation on earthquake ductility requirements*. 1st ed., 134. Berkeley: University of California.
Cogurcu, M. T. 2015. Construction and design defects in the residential buildings and observed earthquake damage types in Turkey. *Natural Hazards and Earth System Science* 15 (4): 931–45. doi: 10.5194/nhess-15-931-2015.
Damcı, E., R. Temur, G. Bekdaş, and B. Sayin. 2015. Damages and causes on the structures during the October 23, 2011 Van earthquake in Turkey. *Case Studies in Construction Materials* 3 (2015): 112–31. doi: 10.1016/j.cscm.2015.10.001.
Dirikgil, T., and O. Atas. 2019. Experimental investigation of the performance of diagonal reinforcement and CFRP strengthened RC short columns. *Composite Structures* 223 (2019): 110984. doi: 10.1016/j.compstruct.2019.110984.
Elnashai, A. S. 2000. Analysis of the damage potential of the Kocaeli (Turkey) earthquake of 17 August 1999. *Engineering Structures* 22 (7): 746–54. doi: 10.1016/S0141-0296(99)00104-2.
Elnashai, A. S., and R. Pinho. 1998. Repair and retrofitting of RC walls using selective techniques. *Journal of Earthquake Engineering* 2 (4): 525–68. doi: 10.1080/13632469809350334.
Erdem, I., U. Akyuz, U. Ersoy, and G. Ozcebe. 2006. An experimental study on two different strengthening techniques for RC frames. *Engineering Structures* 28 (13): 1843–51. doi: 10.1016/j.engstruct.2006.03.010.
FEMA 356. 2000. *NEHRP guidelines for the seismic rehabilitation of buildings*. Washington, DC: Federal Emergency Management Agency.
Frosch, R. J., W. Li, J. O. Jirsa, and M. E. Kreger. 1996. Retrofit of non-ductile moment-resisting frames using precast infill wall panels. *Earthquake Spectra* 12 (4): 741–60. doi: 10.1193/1.1585908.
Furuta, T., T. Kanakubo, and H. Fukuyama. 2003. Evaluation of shear capacity of RC columns strengthened by continuous fiber. Proceedings of the 6th International Conference on Fiber Reinforced Polymers for Reinforced Concrete Structures, (FRPRCS-6), 507–16, Singapore.
Ghobarah, A., A. Biddah, and M. Mahgoub. 1997. Seismic retrofit of reinforced concrete columns using steel jackets. *European Earthquake Engineering* 11 (2): 21–31.
Ghosh, K. K., and S. A. Sheikh. 2007. Seismic upgrade with carbon-fiber reinforced polymer of columns containing lap-spliced reinforcing bars. *ACI Structural Journal* 104 (2): 227–36.
Görgülü, T., Y. S. Tama, S. Yilmaz, H. Kaplan, and Z. Ay. 2012. Strengthening of reinforced concrete structures with external steel shear walls. *Journal of Constructional Steel Research* 70 (2012): 226–35. doi: 10.1016/j.jcsr.2011.08.010.
Gunes, O. 2015. Turkey's grand challenge: Disaster-proof building inventory within 20 years. *Case Studies in Construction Materials* 2 (2015): 18–34. doi: 10.1016/j.cscm.2014.12.003.
Harris, H. G., and G. Sabnis. 1999. *Structural modelling and experimental techniques*. 2nd ed., Chapter: 2, 37. Boca Raton: CRC Press LLC.
Hassan, A. F., and M. A. Sozen. 1997. Seismic vulnerability assessment of low rise buildings in regions with infrequent earthquakes. *ACI Structural Journal* 94 (1): 31–39.
Ismaeil, M. A., and A. E. Hassaballa. 2013. Seismic retrofitting of a RC building by adding steel plate shear walls. *IOSR Journal of Mechanical and Civil Engineering (IOSR-JMCE)* 7 (2): 49–62. doi: 10.9790/1684-0724962.
Kaltakci, M. Y., M. H. Arslan, and U. S. Yilmaz. 2011. Experimental and analytical analysis of RC frames strengthened using RC external shear walls. *Arabian Journal for Science and Engineering* 36: 721–47. doi: 10.1007/s13369-011-0074-4.
Kucukgoncu, H. 2018. An experimental study of analyzing the seismic behavior of strengthened three dimensional frame structure. Ph.D. Thesis, Erciyes University Graduate School of Natural and Applied Science in Turkey. [In Turkish].
Martinelli, A., G. Cifani, G. Cialone, L. Corazza, and G. Petrucci. 2008. Building vulnerability assessment and damage scenarios in Celano (Italy) using a quick survey data-based methodology. *Soil Dynamics and Earthquake Engineering* 28 (10–11): 875–89. doi: 10.1016/j.soildyn.2008.03.002.

Menoni, S. 2001. Chains of damages and failures in a metropolitan environment: Some observations on the Kobe earthquake in 1995. *Journal of Hazardous Materials* 86 (1–3): 101–19.
Miura, H., S. Midorikawa, K. Fujimoto, B. M. Pacheco, and H. Yamanaka. 2008. Earthquake damage estimation in Metro Manila, Philippines based on seismic performance of buildings evaluated by local experts' judgments. *Soil Dynamics and Earthquake Engineering* 28 (10–11): 764–77. doi: 10.1016/j.soildyn.2007.10.011.
Moehle, J. P. 2000. State of research on seismic retrofit of concrete building structures in the US. Proceeding of US–Japan symposium and Workshop on Seismic Retrofit of Concrete Structures — State of Research and Practice, USA.
Oehlers, D. J. 1990. Strengthening reinforced concrete beams by bonding steel plates to their soffits. 2nd National Structural Engineering Conference, Barton, ACT: Institution of Engineers, Vol. 90 (10), 346–50, Australia.
Ozcan, O., B. Binici, and G. Ozcebe. 2008. Improving seismic performance of deficient reinforced concrete columns using carbon fiber-reinforced polymers. *Engineering Structures* 30 (6): 1632–46. doi: 10.1016/j.engstruct.2007.10.013.
Ozturk, M. 2010. Strengthening of reinforced concrete frames of insufficient earthquake resistance by applying external shear wall with coupling beam. Ph.D. Thesis, Selcuk University Graduate School of Natural and Applied Science in Turkey. [In Turkish].
Park, H., and T. Eom. 2004. Energy dissipation capacity of flexure-dominated reinforced concrete members. Proceedings of the 13th World Conference on Earthquake Engineering, Vancouver, Canada, Paper No. 3481.
Phan, L. T., G. S. Cheok, and D. R. Todd. 1995. Strengthening methodology for lightly reinforced concrete frames: Recommended design guidelines for strengthening with infill walls. Building and Fire Research Laboratory National Institute of Standards and Technology, Gaithersburg, MD, NISTIR 5682, July.
Pujol, S., and D. Fick. 2010. The test of a full-scale three-story RC structure with masonry infill walls. *Engineering Structures* 32 (10): 3112–221. doi: 10.1016/j.engstruct.2010.05.030.
Saadatmanesh, H., M. R. Ehsani, and M. W. Li. 1994. Strength and ductility of concrete columns externally reinforced with fiber composite straps. *ACI Structural Journal* 91 (4): 434–47.
Sezer, H., A. S. Whittaker, K. J. Elwood, and K. M. Mosalam. 2003. "Performance of reinforced concrete buildings during the August 17, 1999 Kocaeli, Turkey earthquake, and seismic design and construction practice in Turkey. *Engineering Structures* 25 (1): 104–14. doi: 10.1016/S0141-0296(02)00121-9.
Sharma, K., L. Deng, and C. C. Noguez. 2016. Field investigation on the performance of building structures during the April 25, 2015, Gorkha earthquake in Nepal. *Engineering Structures* 121 (2016): 61–74. doi: 10.1016/j.engstruct.2016.04.043.
Sonuvar, M. O., G. Ozcebe, and U. Ersoy. 2004. Rehabilitation of reinforced concrete frames with reinforced concrete infills. *ACI Structural Journal* 101 (4): 494–500.
Spadea, G., F. Bencardino, and R. N. Swamy. 1998. Structural behavior of composite RC beams with externally bonded CFRP. *ASCE Journal of Composite Construction* 2 (3): 132–37. doi: 10.1061/(ASCE)1090-0268(1998)2:3(132).
Spence, R., J. J. Bommer, R. D. Del, J. Bird, N. Aydinoglu, and S. Tabuchi. 2003. Comparing loss estimation with observed damage: A study of the 1999 Kocaeli Earthquake in Turkey. *Bulletin of Earthquake Engineering* 1 (2): 83–113. doi: 10.1023/A:1024857427292.
Takeda, T., M. A. Sozen, and N. N. Nielsen. 1970. Reinforced concrete response to simulated earthquakes. *ASCE Journal of Structural Engineering* 96 (12): 2557–73.
TEC 2007. 2007. *Turkish earthquake code, regulations on buildings to be constructed in seismic zones*. Ankara: Ministry of Public Works and Settlement.
Türk, M., U. Ersoy, and G. Özcebe. 2003. Seismic rehabilitation of RC frames with RC infill walls. The Proceedings of 5th National Conference on Earthquake Engineering, İstanbul, Turkey, CD-ROM Paper No. AT-045.
Tzoura, E., and T. C. Triantafillou. 2016. Shear strengthening of reinforced concrete T-beams under cyclic loading with TRM or FRP jackets. *Material Structures* 49 (1): 17–28. doi: 10.1617/s11527-014-0470-9.
Ünal, A. 2012. Strengthening of reinforced concrete frames not designed according to TDY 2007 with out of plane external shear wall. MS Thesis, Selcuk University Graduate School of Natural and Applied Science in Turkey. [In Turkish].
Yakut, A., P. Gülkan, B. S. Bakır, and M. T. Yılmaz. 2005. Re-examination of damage distribution in Adapazarı: Structural considerations. *Engineering Structures* 27 (7): 990–1001. doi: 10.1016/j.engstruct.2005.02.001.
Ye, L., Q. Yue, S. Zhao, and Q. Li. 2002. Shear strength of reinforced concrete columns strengthened with carbon-fiber-reinforced plastic sheet. *ASCE Journal of Structural Engineering* 128 (12): 1527–34. doi: 10.1061/(ASCE)07339445-(2002)128:12(1527).
Yön, B., E. Sayın, and O. Onat. 2017. Earthquakes and structural damages, earthquakes-tectonics. *Hazard and Risk Mitigation Intech Open* 13: 319–39. doi: 10.5772/65425.